ACS OMEGA

Open Access

http://pubs.acs.org/journal/acsodf

Article

Heterogeneous Calcium Oxide Catalytic Filaments for Three-Dimensional Printing: Preparation, Characterization, and Use in Methyl Ester Production

Kritsakon Pongraktham and Krit Somnuk*

Cite This: *ACS Omega* 2024, 9, 27578−27591

Read Online

ACCESS | Metrics & More | Article Recommendations

ABSTRACT: This study aimed to investigate heterogeneous catalytic filaments of calcium oxide (CaO) for fused deposition modeling three-dimensional (3D) printers. The CaO catalysts were blended with acrylonitrile butadiene styrene (ABS) plastic to form catalytic filaments. A single-screw filament extruder was used to prepare the filaments, following which their mechanical properties, thermal properties, morphology, catalytic characteristics in biodiesel production, and reusability were evaluated. In accordance with the results, a maximum CaO catalyst content of 15 wt % was recommended to be blended in the ABS pellet. The hardness and compressive strength of these catalytic filaments were shown to be improved. Subsequently, the catalytic filaments with the highest CaO content (15 wt %) were used to produce methyl ester from pretreated sludge palm oil through the transesterification process. To determine the recommended conditions for achieving the highest purity of methyl ester in biodiesel, the process parameters were optimized. A methyl ester purity of 96.58 wt % and a biodiesel yield of 79.7 wt % could be achieved under the recommended conditions of a 9.0:1 methanol to oil molar ratio, 75.0 wt % catalytic filament loading, and 4.0 h reaction time. Furthermore, the reusability of the 15 wt % CaO catalytic filaments was evaluated in a batch process with multiple transesterification cycles. The results indicated that the purity of methyl ester dropped to 95.0 wt % only after the fourth cycle. The method used in this study for preparing and characterizing CaO catalytic filaments can potentially serve as a novel approach for constructing biodiesel reactors using 3D printing technology.

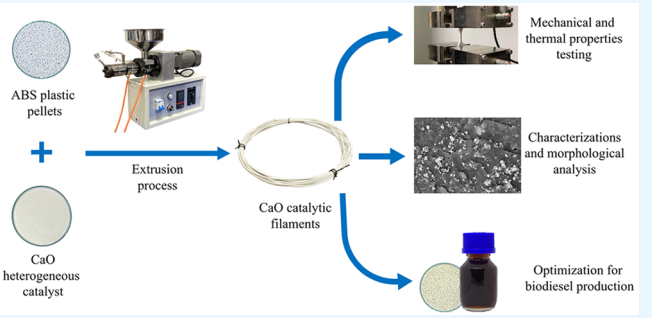

1. INTRODUCTION

Biodiesel can be produced via transesterification using low levels of free fatty acids (FFAs) and fats with alcohol and a base catalyst.[1] After the reaction is complete, fatty acid methyl ester (FAME) and glycerol are formed. However, when attempting to produce high-purity biodiesel from raw materials with high FFA concentrations, it is generally recommended to conduct esterification as a pretreatment step prior to the transesterification process.[2] Raw materials contribute significantly to the overall cost of biodiesel production. Edible oils such as palm, sunflower, soybean, and rapeseed oils have been traditionally used as substrates in feedstocks for commercial biodiesel production.[3] However, there have been growing concerns regarding the use of edible vegetable oil as an energy source, as it competes with its use as a food source.[4] To address these concerns, biodiesel producers have been actively exploring alternative sources of raw materials, particularly nonedible oils such as jatropha, rubber seed, neem, sewage sludge, and waste cooking oils.[5] This push has resulted from the desire to find cost-effective, sustainable feedstocks that also address food security issues.[4] In this regard, the palm oil mill plants in Thailand generate a byproduct called sludge palm oil (SPO). SPO is a viscous and semisolid substance containing a high level of organic matter. Due to its low cost and significant organic FFA content, this waste material from the settling ponds presents a promising option as an energy source.[6]

To achieve both high yields and high purity of FAME during the biodiesel production process, the catalyst plays a crucial role in accelerating the reaction. The most commonly used, commercially available, homogeneous catalysts for biodiesel production via transesterification are sodium hydroxide (NaOH) and potassium hydroxide (KOH), both of which are soluble in the reaction mixture. These catalysts offer several advantages over heterogeneous catalysts, such as shorter reaction times and lower chemical consumption.[7] However,

Received: March 30, 2024
Revised: April 24, 2024
Accepted: June 6, 2024
Published: June 12, 2024

Table 1. Comparing the Use of CaO Solid Catalyst in the Biodiesel Production Process

Feedstock	Catalyst	Methanol to oil molar ratio	Catalyst loading (wt %)	Reaction time (h)	Temperature (°C)	Reusability (cycle)	Methyl ester	Ref
Canola oil	Na−K/CaO	9:1	3	3	50	4	97.6%	Khatibi et al.[25]
Mongongo nut oil	CaO nanoparticles	9:1	12	3	65	–	85 wt %	Mmusi et al.[13]
Palm oil	CaO/ZrO2	9:1	6	1	65	3	96.99%	Li et al.[11]
Soybean oil	Waste snail shell CaO	8:1	6	3	70	7	96.11%	Das et al.[26]
Sunflower oil	CaO/biochar[a]	15.6:1	7.3	5	99.5	3	99.5%	Di Bitonto et al.[14]
Sunflower oil	Waste scallop seashells CaO	12:1	10	4	65	4	97%	Nahas et al.[10]
Waste cooking oil	Grooved razor shell CaO	15:1	5	3	65	6	94%	Aitlaalim et al.[27]
Waste edible oil	CaO/MgO	16.7:1	4.5	7	69	6	98.37%	Foroutan et al.[28]
PSPO	CaO/ABS catalytic filament[b]	9:1	75	4	50	4	96.58 wt %	This study

[a]20% CaO/biochar.[14] [b]75 wt % catalytic filament loading (consisting of 15 wt % CaO catalyst and ABS plastic) based on the initial weight of PSPO.

the impracticality of removing these catalysts from the reaction mixture is a major drawback. More wastewater is generated during the purification process required to remove the homogeneous catalyst from the crude biodiesel using the washing method. Therefore, it becomes essential to treat highly alkaline wastewater before discharging it into the environment; however, this results in an increase in the overall cost of the treatment procedure.[8] On the other hand, heterogeneous or solid catalysts do not need to be cleaned with water and have been proposed as a solution to address the treatment-related challenges of homogeneous catalysts, as they are easier to separate and recover from the reaction mixture. Additionally, they are chemically cost-effective because they may be regenerated for subsequent reactions.[9] Heterogeneous base catalysts, including single alkaline earth metal oxides,[10] mixed metal oxides,[11] and supported alkali metal,[12] have shown promising potential as effective catalysts for the transesterification reaction in biodiesel production.[9] However, calcium oxide (CaO) is the most commonly utilized heterogeneous base catalyst for converting glycerides to ester, because of its lower cost, lower toxicity, and simpler synthesis of the calcite structure.[13] Nahas et al.[10] studied biodiesel production from waste cooking oil using a CaO solid catalyst from waste scallop seashells. The results showed that 97% biodiesel was achieved under the conditions of 12:1 methanol to oil molar ratio, 10 wt % catalyst loading, and 4 h reaction time. Moreover, the catalyst demonstrated excellent stability even after four reaction cycles. They suggested that this catalyst is promising for industrial applications and for scaling up biodiesel production schemes.[10] In the state of the art of using CaO-based heterogeneous catalysts, di Bitonto et al.[14] suggested that the use of CaO supported onto biochar showed efficient promotion of the transesterification process. This approach also results in easier recovery and reusability of conventional CaO solid catalysts, improving its overall efficiency.[14] Table 1 lists a comparison of using CaO heterogeneous catalysts in the production of biodiesel. The literature suggests that a methanol to oil molar ratio between 8:1 to 16.7:1, catalyst contents of 3 to 12 wt %, and a reaction time of 1 to 7 h have been utilized to produce biodiesel from various feedstocks with more than 85% biodiesel purity obtained. These catalysts can also be reused for at least three cycles. Therefore, the use of the CaO solid catalyst was recommended over homogeneous catalysts due to its superior performance, cleanliness, reusability, lower solubility, ease of handling, and environmental friendliness.

The state-of-the-art technique known as additive manufacturing or three-dimensional (3D) printing can be used to generate 3D models using computer-aided design (CAD) software. The use of 3D printing technology offers several benefits, including enhanced conceptual adaptability, cost-effective manufacturing processes, and faster prototyping capabilities.[15] As a result, it has immense potential for a wide range of industries, including dentistry, food processing, automobile manufacturing, architecture, education, engineering, robotics, and aerospace.[16] In the fused deposition modeling (FDM) printing method, commercial thermoplastics, such as polylactic acid (PLA), acrylonitrile butadiene styrene (ABS), poly(vinyl alcohol) (PVA), and thermoplastic polyurethane (TPU) are primarily used as source materials.[15] To explore the feasibility of augmenting the pure plastic filament used in 3D printing, several studies have investigated the addition of various components. These components include carbon fibers,[17] rubber materials,[18] carbon black particles,[19] organic fibers,[20] and metal powders.[21] The objective of these investigations was to evaluate the mechanical, thermal, electrical, chemical, and physical properties of the resulting composite filaments. While 3D printing techniques have found application in fields such as electrochemistry, analytical chemistry, and biotechnology for improving filaments used in chemical processes,[22] limited research has focused on catalytic filaments for chemical processes. In this context, heterogeneous catalysts are added to plastic filaments during the extrusion process to produce catalytic filaments for use in 3D printers. This implies that catalytic filaments can be employed to construct catalytic reactors, in which a heterogeneous catalyst is integrated into the plastic filament structure of the reactor. When the chemical reactants come into contact with the catalyst on the catalytic reactor, the reactor facilitates the acceleration of chemical processes.[23]

In our previous work,[24] a continuous rotor-stator-type hydrodynamic cavitation reactor for the two-step esterification production process of SPO for biodiesel production from high-FFA raw materials was described. Optimization of five parameters, namely methanol content, sulfuric acid content, diameter of hole, depth of hole, and speed of rotor, was

https://doi.org/10.1021/acsomega.4c03063
ACS Omega 2024, 9, 27578−27591

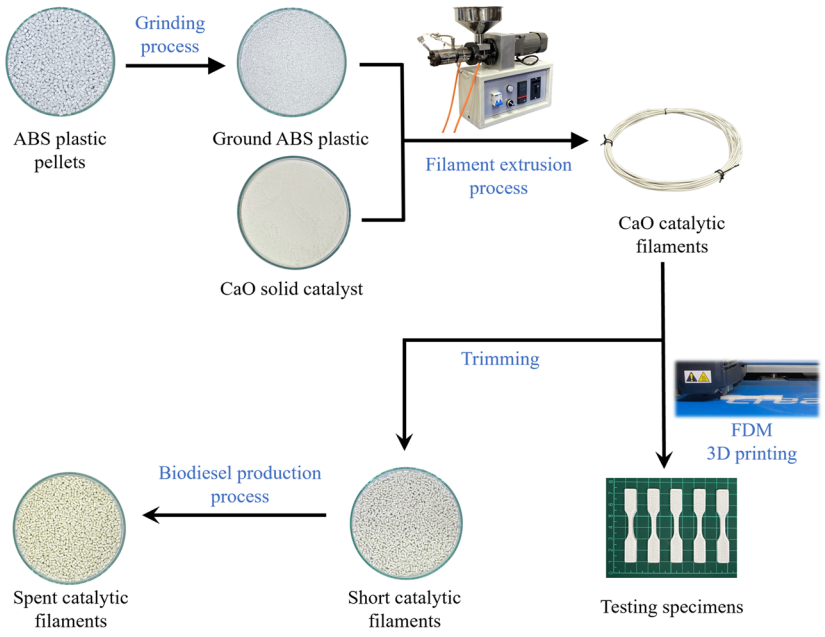

Figure 1. Preparation of CaO catalytic filaments for 3D printing and biodiesel production.

conducted to achieve the lowest FFA content. The actual experiment resulted in a final FFA content of 0.94 wt % and a product yield of pretreated sludge palm oil (PSPO) of 93.9 vol % under two-step acid catalyzed esterification. However, PSPO still contained residual tri-, di-, and monoglycerides having concentrations of 6.93, 2.57, and 0.30 wt %, respectively. Therefore, to achieve high-purity biodiesel, a three-step process involving a transesterification reaction using a base catalyst is recommended. This transesterification reaction helps convert the remaining glycerides in PSPO to methyl esters.[24]

To the best of our knowledge, there have been no reports of extruding and printing CaO catalytic filaments for biodiesel production, as shown in Table 1. As a result, the goal of this study was to investigate CaO catalytic filaments for FDM 3D printing, including their preparation, characterization, and role in methyl ester production from PSPO in a batch process. This involved extruding and printing catalytic filaments containing CaO catalysts at concentrations of 5, 10, and 15 wt % blended with ABS plastic. The study aimed to assess the mechanical (tensile, compressive, and flexural strengths, and hardness), characterization (morphological, composition, specific surface area, and pore diameter), and thermal properties of the catalytic filaments. Additionally, the response surface methodology (RSM) was employed to optimize the production of biodiesel from PSPO using the CaO catalytic filaments by varying three parameters (methanol content, catalytic filament loading, and reaction time). Lastly, the reusability of the catalytic filaments was evaluated in terms of the number of transesterification cycles it could be used for in the batch process.

2. MATERIALS AND METHODS

2.1. Materials. ABS plastic pellets (LG ABS HP171, LG Chem Huizhou, China) were blended with laboratory-grade CaO powder (KemAus, Australia) to produce catalytic filaments for 3D printing. The ABS plastic material was chosen for the purpose of this study because of its superior resistance to chemical reactants such as acid catalysts, base catalysts, and alcohols than to other PLA, PVA, TPU polymers.[29,30] For biodiesel production via transesterification, commercial grade methanol (99.7%) and CaO powder (90.0%) were used as the reactants. Similar to our previous work, the present study used PSPO with a low level of FFAs as the raw material. The oil was obtained from SPO through continuous hydrodynamic cavitation in a two-step esterification process.[24] The main component of the PSPO was 89.25 wt % methyl ester, while the remaining components included 9.79 wt % triglycerides (TG), 0.80 wt % diglycerides (DG), 0.24 wt % monoglycerides (MG), and 0.94 wt % FFA. One of the objectives of this study was to use a base catalytic filament in the transesterification reaction to convert the remaining glycerides (TG, DG, and MG) into high-purity methyl ester. The PSPO had an average molecular weight of 327.1 g/mol, a density of 850 kg/m^3, and a dynamic viscosity of 5.36 cSt at 60 °C.[24] To analyze the composition of the purified biodiesel, thin-layer chromatography with flame ionization detection (TLC/FID; Iatroscan MK-65, Mitsubishi Kagaku Latron Inc., Tokyo, Japan) was used, with quartz−silica gel rods as the stationary phase (Chromarod-S5, LSI Medience Corporation, Tokyo, Japan). For the analytical procedures, the mobile phases used for the development of organic compounds in biodiesel, including methyl ester, TG, DG, MG, and FFA, consisted of hexane, diethyl ether, formic acid, and benzene, all of which were of analytical grade.

2.2. Preparation of Catalytic Filaments for 3D Printing. The process of preparing the catalytic filaments is shown in Figure 1. The ABS pellets were used to make the catalytic filaments. Subsequently, they were dried in an oven at a temperature of 75 °C for 7 h to eliminate any residual moisture. Following the drying process, the ABS pellets were ground using a grinder machine (GM-800S1, OrmiSmart, China) and then sieved with an 18 number mesh (1.0 mm). The catalytic filaments were formed by blending ABS and CaO powders together. They were then transformed into long filaments using a single-screw filament extruder with a water-cooling jacket (Desktop extruder SJ20, RobotDigg, China) using a CaO loading range of 5 to 15 wt %. During the extrusion process, the nozzle diameter was set at 1.75 mm, the

https://doi.org/10.1021/acsomega.4c03063
ACS Omega 2024, 9, 27578−27591

screw was rotated at a speed of 12.5 rpm, and the temperature of the metering zone in the extruder was maintained at 205 °C using a digital temperature controller (AK6, WINPARK, China). The average production capacity was 0.18 kg/h. The extruded material was cooled using an air-cooling fan. The diameter of the catalytic filaments from the extruder was monitored in real time using a digital vernier caliper (TDG50 digital depth gauge, Bartec USA, USA), which was connected to a microcontroller (Mega 2560 R3, Arduino, Italy) for validation purposes. After the extrusion process, the filaments were immediately sealed in zip-lock plastic bags filled with absorbent silica gel to protect them from moisture in the surrounding air. To create printed specimens using 3D printing, the filaments were deposited layer-by-layer using the dual nozzle of a 3D printer (Creator 3, FlashForge, China) via the FDM technique. The printing profiles were as follows: a nozzle diameter of 0.8 mm, a nozzle temperature of 230 °C, a platform temperature of 110 °C, a layer height of 0.4 mm, a base printing speed of 10 mm/s, and 100% plastic infill density.

2.3. Mechanical Properties of Catalytic Filaments. To evaluate the mechanical properties of the catalytic reactor fabricated through 3D printing, various tests including tensile, compression, flexural, and hardness tests were conducted. The weight ratios of CaO to ABS were varied from 0 to 15 wt %. For the tensile tests, specimens in accordance with ASTM D638 type V specimens were used,[31] as shown in Figure 2. These tests were carried out using a universal testing machine (Z010, Zwick/Roell, Germany) equipped with a 1000 N load cell. The hauling speed was set at 1 mm/min, and a gauge length of 9.53 mm was employed.[20] The compression properties were evaluated based on ASTM D695.[32] The specimens used for the compression test had a diameter of 12.7 mm and a length of 25.4 mm.[33] The same universal testing machine was used with a 10000 N load cell and a test speed of 1.3 mm/min. The flexural test was conducted according to the ASTM D790 standard.[34] A different universal testing machine (Z005, Zwick/Roell, Germany) was employed for this experiment. The specimens had a width of 12.7 mm, length of 50.8 mm, and thickness of 1.6 mm.[35] A test speed of 5 mm/min and a support span of 25.4 mm was used, along with a 2500 N load cell. The hardness of the printed workpieces was measured using a hardness tester (Digitest II, Bareiss, Germany)), following the ASTM D2240 shore D standards.[36,37] The analytical tests were performed at a temperature of 23 ± 2 °C and a relative humidity of 50 ± 5%. The average and standard deviation were calculated based on five repetitions for each testing condition.

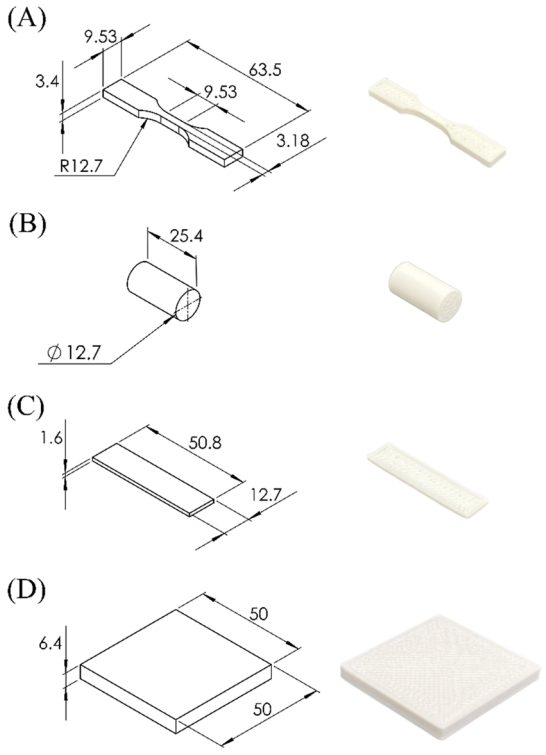

Figure 2. Dimensions of specimens (unit: millimeters) and images of real printed specimens for (A) tensile, (B) compressive, (C) flexural, and (D) hardness testing.

A scanning electron microscope (SEM; SU3900, Hitachi, Japan) was used to observe the dispersion of CaO catalysts in the filaments along the cross-section of the specimens using backscattered electron images obtained under the conditions of a 20 kV accelerating voltage and 1000× magnification. SEM images can provide valuable insights into the physical interaction between the solid catalyst and the ABS material, as well as the crystalline properties of the interface between these two materials.[17] To prepare the samples for testing, the catalytic filaments were submerged in liquid nitrogen and then cut in half. The fractured surfaces of the filaments were then examined under the SEM after undergoing a gold-coating procedure. This analysis aimed to provide a clear understanding of the morphological characteristics of the catalytic filaments.[20]

2.4. Determination of Catalytic Filament Characteristics. The structure and characteristics of the catalytic filament were analyzed using an X-ray diffractometer (XRD). The testing sample was 3D printed into a cylinder with a 32 mm diameter and 4 mm thickness to fit the sample holder. The X-ray diffractogram was obtained via an X-ray diffractometer (Empyrean, Malvern Panalytical, Netherlands) with a Cu tube. The analysis was maintained at 40 kV voltage, 30 mA current, 0.154 nm wavelength, 5−90° scan range (2θ), 0.026° step size, and 70.125 s time/step. The specific surface area and average pore diameter of the fresh catalytic filaments were examined using an ASAP-2460 surface area and porosimetry analyzer (ASAP-2460, Micromeritics, USA), based on the Brunauer, Emmet, and Teller (BET) method. Their surface was analyzed using the static volumetric N_2 absorption method at a constant temperature of −196.85 °C, with degassing temperatures at 70 °C.[6]

2.5. Analysis of Thermal Characteristics. The thermogravimetric analysis (TGA) and differential scanning calorimetry (DSC) of the catalytic filaments were performed using a thermogravimetric analyzer (TGA/DSC3+, Mettler Toledo, Switzerland). The TGA measurements were performed within a temperature range of 30 to 600 °C, with a heating rate of 10 °C/min, under an inert nitrogen gas environment with a flow rate of 50 mL/min. This method evaluates the stability of the composite materials and quantifies the weight loss caused by degradation at high temperatures.[38] For DSC, the temperature range was set between 30 and 250 °C, with all other parameters the same as in the TGA analysis. DSC analysis was used to determine the changes in the heat flux of the composite materials over a range of temperatures, providing valuable insights into their thermal properties and behavior under various conditions.[38] The glass transition temperature

https://doi.org/10.1021/acsomega.4c03063
ACS Omega 2024, 9, 27578−27591

(T_g) is the point of phase changes in polymers, transitioning from a glassy to a rubbery state.[18] However, ABS, being a thermoplastic polymer with an amorphous nature, lacks a distinct melting point. Instead, it gradually softens with increasing temperature until it reaches a liquid state. Consequently, ABS does not exhibit a true melting peak but rather a melting range of temperatures that can be considered between 190 and 230 °C.[39] These temperature ranges can serve as references for estimating the temperatures within the printing bed, nozzle, and extruder during the 3D printing process using catalytic filaments.

2.6. Biodiesel Production Using Catalytic Filaments.

2.6.1. Experimental Procedure. The performance of the CaO catalytic filaments in biodiesel production was assessed through laboratory-scale experiments. The investigation aimed to evaluate the influence of various parameters including the methanol to oil molar ratio, catalytic filament loading, and reaction time on the purity of methyl ester, as presented in Table 2. Long extruded catalytic filaments were trimmed to short filaments, with an average diameter of 1.8 mm and length of 4.5 mm and weighing 12 mg for batch transesterification. The PSPO feedstock for the transesterification reaction was obtained from the two-step esterification process of SPO using a hydrodynamic cavitation reactor, as detailed in a previous paper.[24] To prepare for the transesterification process using short catalytic filaments, 30 g of PSPO and methanol were heated to 50 °C and agitated at 500 rpm in a beaker using a magnetic stirrer (B S104, RCT basic, IKA, Germany). A digital thermometer (51 II, Fluke, China) was used to monitor the temperature of the mixture. The catalytic filament loading consists of 15 wt % CaO content in the weight of ABS plastic materials, which was used to test in all experiments. A parameter of catalytic filament loading (concentration of 15 wt % CaO/ABS) refers to the weight of catalytic filaments with respect to the weight of the initial PSPO. The PSPO, methanol, and catalytic filaments were continuously stirred according to the experimental design matrix presented in Table 3 until the desired reaction time was reached. After the reaction, the catalytic filaments in the mixture were separated using a filter sieve and then subjected to centrifugation at 4000 rpm for 5 min using a centrifuge device (DM0412, DLAB, China). The samples were subsequently washed with warm water to remove any remaining methanol and catalyst before being sent to a TLC/FID analyzer to determine the purity of methyl ester, TG, DG, MG, and FFA.

Table 2. Code Levels of Independent Variables

		Code levels				
Independent variables	Units	−1.682	−1	0	+1	+1.682
Methanol to oil molar ratio (M)	molar ratio	4	6	9	12	14
Catalytic filament loading (C)	wt %	33	50	75	100	117
Reaction time (t)	h	0.6	2	4	6	7.4

2.6.2. Design of Experiments. The effects of three key factors on the purity of methyl esters: the methanol to oil molar ratio ranging from 4−14, the catalytic filament concentration ranging from 33−117 wt %, and the reaction time ranging from 0.6−7.4 h. These independent variables were transformed into five coded levels (−1.682, −1, 0, +1, and +1.682) using a central composite design with an inscribed mode,[2] as shown in Table 2. A total of 18 experimental conditions were established by varying these three parameters. The resulting methyl ester purity data were included as the response parameter in the experimental design matrix, as indicated in Table 3. The relationship between each independent variable and its interactions with the dependent variable was determined using RSM, by employing a quadratic equation (eq 1).[40] The statistical significance of each independent variable was assessed through the calculation of *p*-values. Any terms with *p*-values exceeding 0.05 in the predictive model were considered to have low significance and thus removed.[6] To validate the predictive model, analysis of variance (ANOVA) was performed at a 95% confidence level using the Microsoft Excel Solver add-in. This analysis was performed to confirm the statistical influence between the predictive model and the experimental data.[2] Subsequently, the model was utilized to compute the highest purity as well as the required minimum value of 96.5 wt % for methyl ester purity. Contour plots generated from the predictive model were used to represent the relationships between methyl ester purity and the three independent variables, illustrating the effects of these independent factors on the dependent variable.

Table 3. Experimental Design Matrix[a]

Run	Methanol to oil (molar ratio)	Catalytic filament loading (wt %)	Reaction time (h)	Methyl ester (wt %)
1	4	75	4.0	92.91
2	6	50	2.0	92.40
3	6	50	6.0	93.95
4	6	100	2.0	93.74
5	6	100	6.0	95.29
6	9	33	4.0	94.08
7	9	75	0.6	93.80
8	9	75	4.0	96.56
9	9	75	4.0	96.60
10	9	75	4.0	96.57
11	9	75	4.0	96.57
12	9	75	7.4	96.62
13	9	117	4.0	95.80
14	12	50	2.0	94.44
15	12	50	6.0	96.02
16	12	100	2.0	95.13
17	12	100	6.0	96.61
18	14	75	4.0	95.80

[a]Note: The molar ratio of methanol to oil was calculated based on the average molecular weight of PSPO, which is 327.1 g/mol.

$$y = \beta_0 + \sum_{i=1}^{k} \beta_i x_i + \sum_{i=1}^{k} \beta_{ii} x_i^2 + \sum_{i=1}^{k} \sum_{j=i+1}^{k} \beta_{ij} x_i x_j + \varepsilon \quad (1)$$

Here, y is the dependent variable and is referred to as purity of methyl ester in this study (wt %), β_0 is the equation constant, k is the number of independent variables, $\beta_i x_i$ is the main effect term, $\beta_{ii} x_i^2$ is the quadratic term, $\beta_{ij} x_i x_j$ is the interaction term, and ε represents the error.

2.6.3. Reusability Analysis of Catalytic Filaments. In comparison to homogeneous catalysts, heterogeneous catalysts offer the advantage of being reusable for multiple cycles. Solid catalysts have the potential to be reused, which can lead to cost reduction in the treatment process, minimized catalyst waste, and reduction in overall production cost.[10] To determine the number of cycles the filaments could be reused for, this study

https://doi.org/10.1021/acsomega.4c03063
ACS Omega 2024, 9, 27578−27591

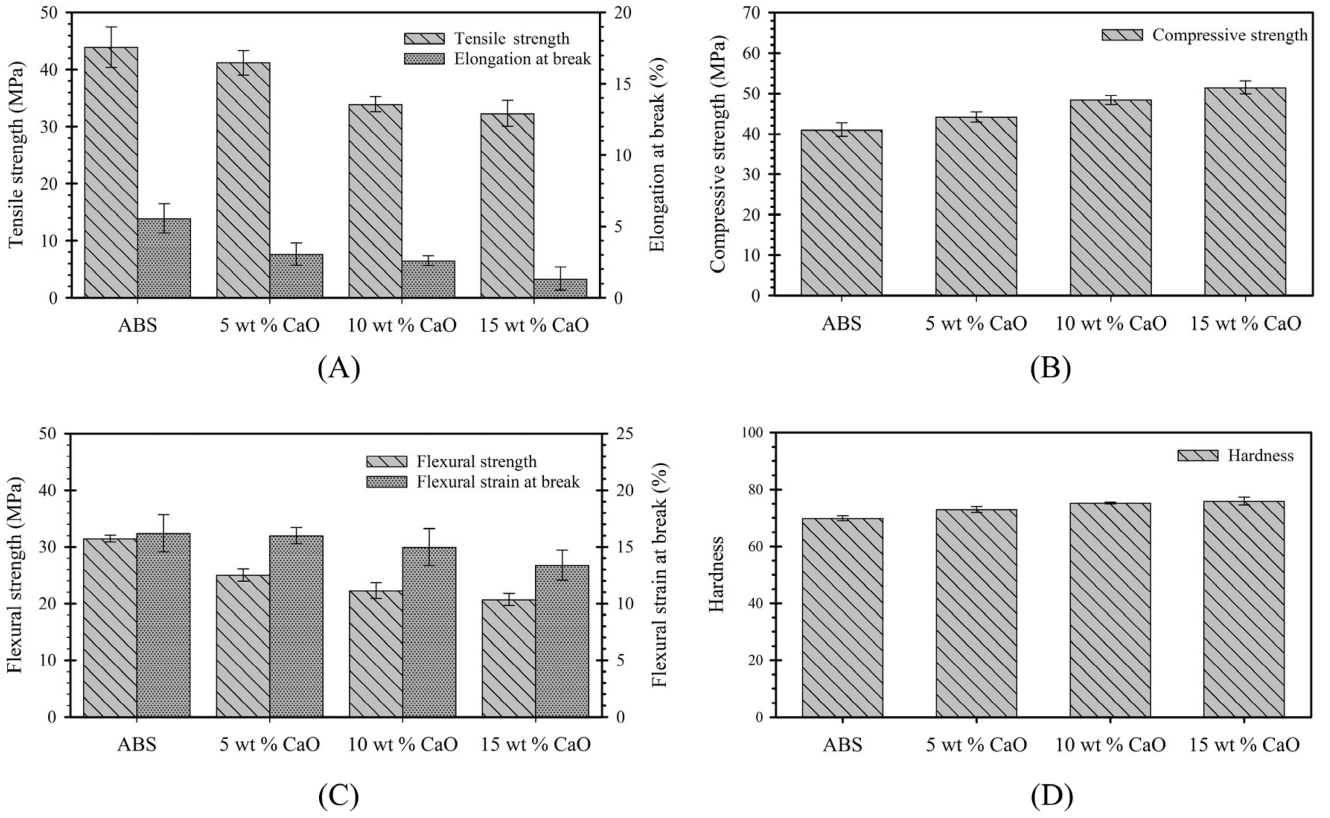

Figure 3. Mechanical properties of catalytic filaments: (A) tensile strength and elongation at break, (B) compressive strength, (C) flexural strength and flexural strain at break, and (D) hardness of ABS and CaO catalytic filaments.

focused on the transesterification process using reused catalytic filaments with the highest CaO concentration of 15 wt %. New catalytic filaments were initially used in the first production cycle. After the biodiesel production process, the catalytic filaments were recovered for further transesterification, termed as the recovery process. During this process, the catalytic filaments were separated through a filter sieve. The used filaments were then washed with methanol in a beaker at 300 rpm for 5 min to remove the oil. Subsequently, the recovered filaments were dried in a hot air oven (UM 200, Memmert, Germany) at 40 °C for 4 h. To explore an alternative to using spent catalytic filaments for each new reaction, the dried recovered catalytic filaments were repeatedly employed for transesterification reactions in subsequent batches of fresh PSPO. After each transesterification cycle, the purity of the methyl ester was analyzed and compared to earlier results to ensure consistency in the purity throughout the reuse of the catalytic filaments. To check the percentages of catalyst weight losses in biodiesel samples, the residual catalytic filaments were filtered using filter paper (Genuine Whatman No. 1 (11 μm); W. & R. Balston, Kent, UK). The residual catalytic (wt %) was calculated by the weight of catalyst losses in biodiesel samples (g) with respect to the weight of initial catalytic filament loading (g), which relates to 100 wt % of initial catalytic filament loading. The leaching of the calcium into the biodiesel product was determined using an inductively coupled plasma optical emission spectrometry[41] (ICP-OES; Avio 500, PerkinElmer, USA) analyzer.

3. RESULTS AND DISCUSSION

3.1. Mechanical Properties of Catalytic Filaments.

The single-screw filament extruder was used to extrude mixtures of CaO and ABS powders into the catalytic filament. Various weight ratios of the CaO catalyst to ABS powders were tested, ranging from 0 to 15 wt %. The maximum allowable weight percentage of the CaO catalyst blended with the ABS powder should not exceed 15 wt% due to the limitations in the extrusion process. Concerns about the addition of more additives to ABS have been raised by Osman and Atia.[20] In their study, they found that modified ABS filaments became more brittle when rice straw fibers were added at concentrations higher than 20%.[20] Moreover, preliminary investigations have revealed that the use of a 20 wt % CaO catalyst mixed with ABS was unsuccessful, as the high CaO concentration hindered melting during the extrusion process through the nozzle. Hence, it is not recommended to use a 20 wt % CaO catalytic filament for forming CaO catalytic filaments using a filament extruder.

3.1.1. Tensile Testing of Catalytic Filaments. The tensile characteristics of the catalytic filament were tested using ASTM D638 type V specimens. The tensile strength of pure ABS was 43.9 MPa. In the catalytic filament, a maximum tensile stress of 41.2 MPa was achieved with a CaO catalyst loading of 5 wt %. However, increasing the CaO catalyst loading resulted in a significant reduction in tensile strength to 34.0 and 32.3 MPa for 10 wt % and 15 wt % loadings, respectively, as shown in Figure 3A. The tensile strength of the CaO catalytic filaments decreased by 6.2%, 22.7%, and 26.4% for 5, 10, and 15 wt % CaO loadings, respectively, compared to that of the pure ABS filament. The decrease in tensile strength

https://doi.org/10.1021/acsomega.4c03063
ACS Omega 2024, 9, 27578−27591

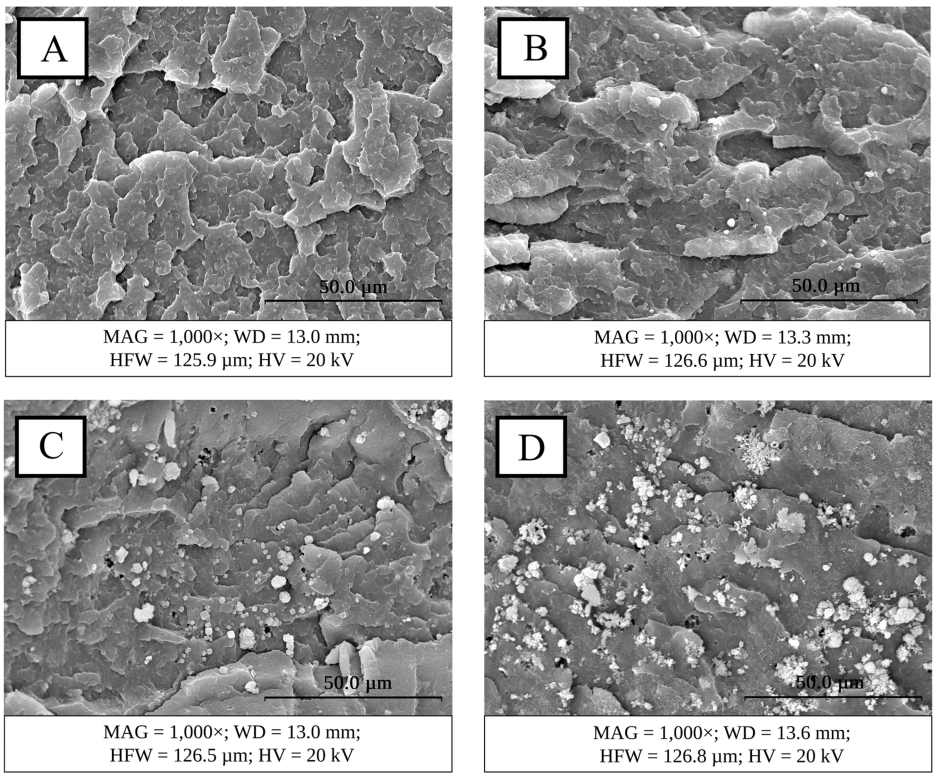

Figure 4. Cross-section morphological images of extruded filaments: (A) pure ABS filament; catalytic filaments with (B) 5 wt %, (C) 10 wt %, and (D) 15 wt % CaO. (MAG is magnification, WD is working distance, HFW is horizontal field width, and HV is accelerating voltage).

can be attributed to the heterogeneous mixing of CaO powders in the plastic filament, which may have reduced adhesion between plastic structures and lowered tensile strength. Another factor that could contribute to these issues is the high material shrinkage during the layer-by-layer 3D printing process, as it affects the mechanical properties.[33] In terms of elongation at break, it was observed that the elongation at break decreased by 45.0%, 53.2%, and 75.8% for CaO loadings of 5, 10, and 15 wt %, respectively, when compared to ABS, as shown in Figure 3A. The decrease in elongation can be attributed to poor interfacial adhesion and the agglomeration of CaO particles and ABS.[42] In addition, a high concentration of CaO in the particles has an effect on stress concentrators, leading to a reduction in the composite's elongation.[43] This problem has been reported previously by Revert et al.,[43] who investigated the influence of adding brewer's spent grain to polypropylene (PP) plastic on the mechanical characteristics of composite. Their results showed that the addition of waste solid particles reduced both the tensile strength and elongation at break of PP composites. When the filler content was increased to 40%, the tensile strength and elongation at break of the composites were reduced to 19 MPa and 6%, respectively. In contrast, PP without solid particles exhibited a tensile strength of 22.7 MPa and an elongation at break of 800%.[43] In conclusion, the addition of CaO catalysts to the plastic filament not only affected the tensile strength but also the elongation at break of the catalytic filaments.

3.1.2. Compressive Testing of Catalytic Filaments. The maximum compressive stress of the catalytic filament, evaluated in accordance with ASTM D695, is shown in Figure 3B. The addition of CaO to ABS resulted in a slight increase in compressive strength. A loading of 15 wt % CaO led to a maximum compressive stress of 51.5 MPa. Comparing the compressive strengths of CaO catalytic filaments with those of the pure ABS filament, the 5, 10, and 15 wt % CaO loadings resulted in increases of 7.7%, 18.0%, and 25.4%, respectively. A higher CaO content in the plastic can improve its stiffness, thereby enabling the polymer to withstand greater compression stresses.[33] A higher CaO content in ABS blends improves the compressive strength and resistance of the catalytic filament to high pressure when applied to the construction of a chemical reactor.

3.1.3. Flexural Testing of Catalytic Filaments. Figure 3C shows the maximum flexural stress and flexural strain at break for the catalytic filament, with varying weight ratios of CaO catalyst powder. As the amount of the CaO catalyst increased to 15 wt %, there was a slight decrease in flexural strength. Specifically, the flexural strengths of the 5, 10, and 15 wt % CaO loadings were reduced by 20.5%, 29.2%, and 34.1%, respectively, in comparison to pure ABS. In all specimens shown in Figure 3C, the flexural strain at break of ABS combined with different concentrations of the CaO catalyst was lower than that of pure ABS. When compared to pure ABS, the flexural strain at break values decreased by 1.2%, 7.4%, and 17.3% for the 5, 10, and 15 wt % CaO concentrations, respectively. Similar findings were reported by Pavon et al.,[44] who found that the addition of calcium carbonate fillers reduced flexural strength due to insufficient contact between the polymer matrix and filler.[44] Therefore, caution must be exercised when employing high concentrations of CaO in catalytic reactors to prevent deflection and fracture as a result of significantly diminished flexural properties.

3.1.4. Hardness Testing of Catalytic Filaments. The hardness of the catalytic filaments was evaluated according to ASTM D2240 shore D, and the results are shown in Figure

https://doi.org/10.1021/acsomega.4c03063
ACS Omega 2024, 9, 27578−27591

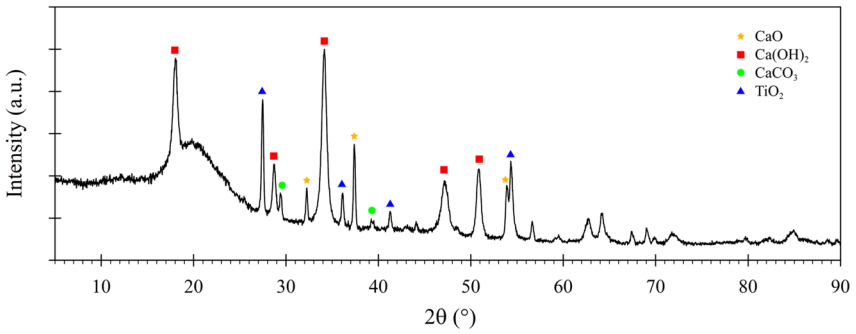

Figure 5. X-ray diffractogram of the 3D-printed CaO catalytic filament.

3D. The hardness of the printed specimens made using CaO catalytic filaments increased by 4.6%, 7.9%, and 8.7% when compared to those made from pure ABS filaments, with CaO loadings of 5, 10, and 15 wt %, respectively. The highest hardness value was observed in the sample containing 15 wt % CaO, with a hardness of 75.9 shore D. These results suggest that the combination of ABS and a CaO catalyst can significantly enhance the hardness of printed models. This finding is consistent with the results reported by Fouly et al.,[45] who stated that the uniform distribution of solid filler particles within the polymeric matrix contributes to increased hardness.[45] Moreover, the addition of CaO powder to increase the relative density of the composite plastic improved the hardness characteristics of the composite plastic, thereby increasing the durability of the catalytic reactor.[44]

3.1.5. Morphological Analysis. Figure 4 shows a comparison of the cross-section fracture surface of the catalytic filaments as observed by the SEM analyzer with different weight ratios of the CaO catalyst. In the case of pure ABS, the SEM images revealed numerous rough surfaces in its morphology, leading to porous structures and a decrease in mechanical properties, as shown in Figure 4A. The addition of CaO catalysts had a significant effect on the surface morphology. The solid CaO catalyst was uniformly distributed across the cross-sectional surface. Smooth fracture surfaces exhibited higher levels of CaO catalyst content due to the presence of catalyst particles, as shown in Figure 4B, C, and D. The mechanical property testing results indicate that this filler enhances the compressive and hardness characteristics of the blended plastic by increasing the relative density.[46] However, a brittle failure mode can also be observed when the solid catalyst content exceeds 10 wt %, resulting in reduced tensile, elongation, and flexural properties due to a lack of cohesion between the solid catalyst and ABS.[33]

3.2. Analysis of Catalytic Filament Properties. *3.2.1. Characterizations of Catalytic Filament.* Figure 5 shows the X-ray diffractogram of the 3D-printed CaO catalytic filament with a 15 wt % blending content. The XRD peak's reflections are consistent with CaO at 32.2°, 37.4°, and 53.9°, indicating that the CaO catalytic filament has the ability to produce biodiesel.[47] The peaks at 18.0°, 28.7°, 34.1°, 47.1°, and 50.8° indicate the presence of calcium hydroxide ($Ca(OH)_2$) phases, showing the hydration nature of CaO. Minor reflections at 29.4° and 39.4° are assigned to calcium carbonate ($CaCO_3$) due to the exposure of fresh CaO in the atmosphere during the extrusion and printing process.[48] Other peaks at 27.4°, 36.1°, 41.2°, and 54.3° pointed to the existence of titanium dioxide (TiO_2), which is present in commercial ABS plastic pellets. The CaO catalytic filament has a BET specific surface area of 0.1182 m^2/g and a large average pore diameter of 14.58 nm. These characteristics make it suitable for use in liquid−solid heterogeneous phase reactions in a mechanical stirrer reactor.[26]

3.2.2. Thermal Stability of Catalytic Filaments. To ensure that the catalytic filaments can be used in the printing process without undergoing thermal decomposition, the temperature for 1% weight loss ($T_{d,1\%}$) was determined by conducting a TGA analysis to identify the initial degradation temperature of the plastic.[38] The analysis results for catalytic filaments containing varying weight ratios of the CaO catalyst are presented in Table 4. The initial degradation temperatures of the catalytic filaments containing 5, 10, and 15 wt % CaO were measured to be 290, 287, and 295 °C, respectively, while pure ABS exhibited an initial degradation temperature of 274 °C. All CaO blending ratios demonstrated high thermal stability up to 270 °C, with no significant weight loss observed for the extruded catalytic filaments. Consequently, the catalytic filaments can be fabricated using 3D printers and extrusion machines without compromising material quality through degradation.[49] After exposure to high temperatures, pure ABS plastic underwent decomposition and left behind only 2.5 wt % of char residues, indicating its low charring ability.[50] The detected glass transition temperature of pure ABS was found to be 107 °C, which is similar to the results reported by Hart et al.[39] For the catalytic filaments, the glass transition temperature was slightly lower than that of pure ABS when higher solid catalyst contents were applied. Specifically, the glass transition temperatures of the catalytic filaments with 5, 10, and 15 wt % CaO contents were 107, 104, and 104 °C, respectively. When CaO particles are dispersed within the ABS matrices, they act as a plasticizer. This results in a reduction in the intermolecular adhesion forces between individual molecules of ABS and consequently leads to lower thermal resistance characteristics. Therefore, the glass transition temperature experiences a slight decrease due to the presence of this dispersed filler in the plastic matrix.[51] The findings of this study suggest that a

Table 4. Thermal Properties of Catalytic Filaments[a]

CaO loading (wt %)	$T_{d,1\%}$ (°C)	T_g (°C)
0 (pure ABS)	274	107
5	290	107
10	287	104
15	295	104

[a]Note: $T_{d,1\%}$ is the initial degradation temperature at 1% weight loss, and T_g is the glass transition temperature.

https://doi.org/10.1021/acsomega.4c03063
ACS Omega 2024, 9, 27578−27591

temperature of 110 °C is suitable for the printing bed to ensure sufficient material adhesion during the printing process.[52]

3.3. Biodiesel Production from PSPO Using Catalytic Filaments. *3.3.1. Experimental Results and Statistical Analysis.* The results of the transesterification process for converting PSPO to methyl ester using 15 wt % CaO catalytic filaments are presented in Table 3. The purity of the methyl ester ranged from 92.40 to 96.62 wt %. After analyzing the results using RSM, the low-significance terms in eq 2 were eliminated by removing those terms in the predictive model with *p*-values greater than 0.05.[6] Consequently, a second-order predictive model with seven terms of eq 2 was derived. Table 5 lists the coefficients and *p*-values of the predictive model for the transesterification process. The statistical analysis indicated that the linear term of methanol (β_1M) had the lowest *p*-value of 9.27×10^{-15}, suggesting that methanol played a significant role in methyl ester production using catalytic filaments. The quadratic term of methanol (β_4M^2), the linear term of the reaction time (β_3t), and the linear term of the catalytic filament (β_2C) ranked second, third, and fourth, respectively, implying that catalytic filament loading and reaction time also have an impact on methyl ester production. The accuracy of the predictive model was evaluated using statistical indicators, with the coefficient of determination (R^2) and the adjusted coefficient of multiple determination ($R^2_{adjusted}$) values being notably high at 0.9994 and 0.9990, respectively. The relationship between the actual purity of methyl ester and the predicted value, shown in Figure 6, confirmed the accuracy of the predictive model. Therefore, this model serves as an accurate and efficient method for evaluating methyl ester purity. In addition, an ANOVA conducted at a 95% confidence level confirmed the statistical validity of the predictive model, as shown in Table 6. The *F*-value (F_0) of 2472.6 obtained from the predictive model using ANOVA exceeded the critical *F*-value of 3.14 ($F_{0.05,\ 7,\ 10}$). Therefore, this model demonstrated statistical significance when estimating methyl ester purity during the biodiesel production using PSPO and CaO catalytic filaments.

Table 5. Coefficients and Statistics of the Predictive Model[a]

Terms	Coefficients	*p*-values
β_0	74.906	1.9038×10^{-21}
β_1	2.0715	9.2688×10^{-15}
β_2	0.18150	1.9445×10^{-13}
β_3	1.3532	1.1277×10^{-13}
β_4	-8.9465×10^{-2}	2.0688×10^{-14}
β_5	-9.3615×10^{-4}	4.3775×10^{-13}
β_6	−0.11947	2.6976×10^{-12}
β_7	-2.3333×10^{-3}	5.3402×10^{-7}

[a]Note: R^2 = 0.9994, and $R^2_{adjusted}$ = 0.9990.

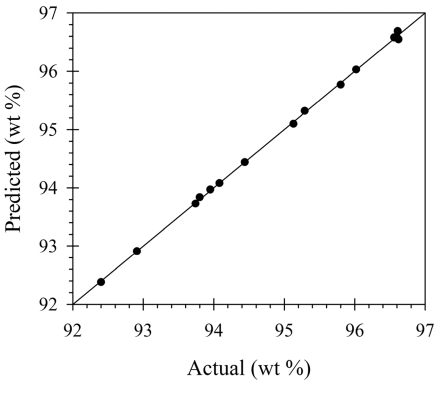

Figure 6. Actual methyl ester purity versus predictive value.

$$ME = \beta_0 + \beta_1 M + \beta_2 C + \beta_3 t + \beta_4 M^2 + \beta_5 C^2 + \beta_6 t^2 + \beta_7 MC \quad (2)$$

3.3.2. Influence of Parameters on the Purity of Methyl Ester. The effects of the methanol to oil molar ratio, catalytic filament loading, and reaction time on the purity of methyl ester were demonstrated through three contour plots. Figure 7A, B illustrates the variations in the methanol to oil molar ratio as a function of the purity of methyl ester. An increase in both methanol concentration and catalytic filament loading resulted in higher methyl ester purities, as shown in Figure 7A. In particular, a methyl ester purity greater than 96.5 wt % was achieved for methanol to oil molar ratios ranging from 8.5:1 and 12.5:1 and catalytic filament loadings ranging from 65 to 105 wt %. As shown in Figure 7B, similar molar ratios (8:1 to 13:1) resulted in methyl ester purities exceeding 96.5 wt %. In accordance with statistical analysis, methanol plays the most significant role in the production of methyl esters. Therefore, the molar ratio of methanol to oil must be carefully prepared to ensure the optimal purity of methyl esters. As the methanol to oil molar ratio increased, the chemical equilibrium shifted toward methyl ester conversion.[14] Additionally, higher amounts of methanol increased the surface area of contact, enhancing the reaction rate and reducing the viscosity of the reaction mixture, thus promoting mass transfer during the mixing process.[48] However, beyond the suitable content of methanol under optimal conditions, a methanol to oil molar ratio exceeding 13:1 could dilute the catalyst and PSPO, both of which are essential for converting glycerides to methyl esters.[10] Similar results have been reported by Gaide et al.,[40] who investigated the performance of synthesized CaO derived from eggshells as a solid catalyst for the transesterification of rapeseed oil with methanol. They observed reduced biodiesel yields due to the reverse reaction of transesterification caused by an excessive methanol to oil molar ratio. They determined that an optimal molar ratio of 10.93:1 methanol to rapeseed oil resulted in a maximum biodiesel yield of 97.8 wt %.[40] Li et al.[11] observed that excessive methanol led to the dilution of the catalyst, resulting in reduced contact between the catalyst and reactants.[11] Hence, careful optimization of the methanol to oil molar ratio is necessary to achieve optimal biodiesel purity. The effects of catalytic filament loading and reaction time on the purity of methyl ester will be discussed in further topics.

The effect of catalytic filaments on methyl ester purities is demonstrated in Figures 7A and C, which illustrate the relationship between catalytic filaments, methanol content, and reaction time. In accordance with the statistical analysis, the loading of catalytic filament is the second most significant factor affecting the purity of methyl ester. As a result, it is necessary to consider the loading of catalytic filament to achieve high purity of methyl ester. The correlation between the purity of methyl ester and the catalytic filament loading is nonlinear due to the reaction nature of heterogeneous catalyst systems that occur between liquid and solid phases.[27] In Figure 7C, a catalytic filament loading ranging from 60 to 110 wt % achieves a methyl ester purity of over 96.5 wt % for a reaction time of 3.5 to 7.4 h, due to an increase in the number of active sites available for the reaction.[53] However, when the catalytic

https://doi.org/10.1021/acsomega.4c03063
ACS Omega 2024, 9, 27578−27591

Table 6. ANOVA Results[a]

Source	Sum of squares	Mean square	F_0	$F_{critical}$	DOF
Regression	33.496	4.7852	2472.6	3.14	7
Residual	0.019353	0.0019353			10
Lack of fit error	0.018453	0.0026361	8.79	8.89	7
Pure error	9.0000×10^{-4}	3.0000×10^{-4}			3
Total	33.515				17

[a]Note: F_0 is the F-value obtained from predictive model, $F_{critical}$ is the critical F-value, and DOF is degrees of freedom.

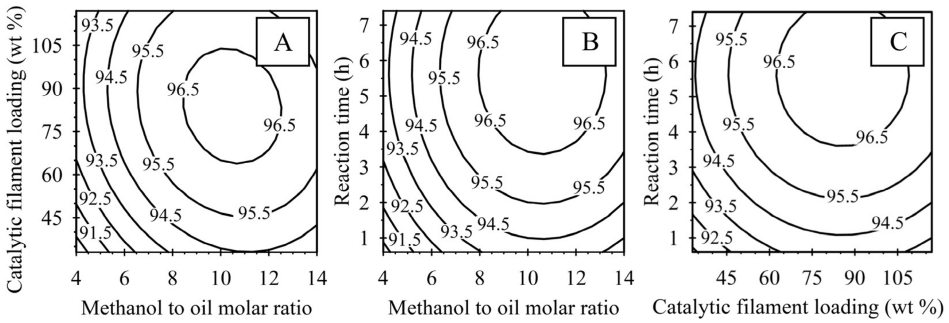

Figure 7. Influence of parameters on the purity of methyl ester: (A) methanol to oil molar ratio and catalytic filament loading, (B) methanol to oil molar ratio and reaction time, and (C) catalytic filament loading and reaction time.

filament loading exceeds 110 wt %, the purity of the methyl ester decreases. This is because a large number of filaments become dense and obstruct the stirrer, leading to decreased mass transfer of mixtures inside the reactor.[54] Similar results were reported by Aisien and Aisien,[55] who investigated the transesterification of rubber seed oil to biodiesel using sulfonated CaO derived from snail shells as a catalyst. They found that exceeding the appropriate catalyst loading resulted in poor reactant diffusion, accumulation, and mass transfer limitations.[55] In conclusion, catalytic filament loading is crucial for enhancing the efficiency and sustainability of biodiesel production processes.

In terms of reaction time, although it ranks third in importance in affecting the purity of methyl ester, careful consideration of the reaction time is required to achieve high purity of biodiesel. The contour plots in Figure 7B, C demonstrate that increasing the reaction time from 0 to 3.5 h enhances the purity of methyl ester. Additionally, a purity of over 96.5 wt % methyl ester could be achieved, with slight increases observed when the reaction time exceeded 3.5 h. Extending the reaction times have been found to improve methyl ester purity by facilitating better mixing and diffusion of solid catalyst and reactants over heterogeneous catalysts.[53] However, the purity of methyl ester may decrease when the reaction time is too long. Similar results were reported by Kirubakaran and Selvan,[47] who synthesized a CaO catalyst from eggshell for biodiesel production from waste chicken fat. They observed a maximum biodiesel yield of 96.7% with a reaction time of 2 h using a nano CaO catalyst. However, when the reaction time was increased beyond 2 h, the biodiesel yield was reduced to 60% due to the presence of equilibrium conditions in the reaction mixture.[47] Das et al.[26] reported that the optimal reaction time for producing biodiesel from soybean oil with CaO derived from waste snail shells is 3 h. Longer reaction times than the optimal duration can have a negative impact because the transesterification reaction is reversible. As reaction time increases, the reaction equilibrium tends to move in a reverse direction. In addition, longer reaction times require more energy and resources for biodiesel production.[26] Therefore, careful operation under the optimal conditions of methanol content, catalytic filament loading, and reaction time is required in order to achieve a highly efficient process with minimal energy and chemical consumption when using CaO catalytic filaments for biodiesel production.

3.3.3. Optimization of Biodiesel Production from PSPO Using Catalytic Filaments. To maximize the purity of methyl ester for biodiesel production from PSPO, the parameters of methanol to oil molar ratio, catalytic filament loading, and reaction time were optimized using RSM. By performing numerical calculations in Microsoft Excel with the solver add-in, the optimal conditions for producing methyl ester of the highest purity, as predicted by model eq 2 were obtained. As shown in Table 7, the optimal conditions for achieving a maximum purity of 97.21 wt % were found to be a methanol to oil molar ratio of 10.5:1, a catalytic filament loading of 83.9 wt

Table 7. Optimal and Recommended Conditions of the Predictive Model[a]

		Conditions	
Variables	Units	Optimal	Recommended
M	molar	10.5	9.0
C	wt %	83.9	75.0
t	h	5.7	4
ME_{model}	wt %	97.21	96.50
ME_{actual}	wt %	96.69	96.58
$Y_{transesterification}$[b]	wt %	77.6	79.7
$Y_{biodiesel}$[c]	wt %	76.2	78.3

[a]Note: M is the methanol to oil molar ratio, C is the catalytic filament loading, t is the reaction time, ME_{model} and $M_{Eactual}$ represent the purity of methyl ester obtained from the predictive model and actual experiment, respectively. [b]$Y_{transesterification}$ (wt %) was calculated by the weight of purified biodiesel (g) with respect to the weight of initial PSPO (g), which relates to 100 wt % of initial PSPO. [c]$Y_{biodiesel}$ (wt %) was calculated by the weight of purified biodiesel (g) with respect to the weight of initial SPO (g), which relates to 100 wt % of initial SPO.

https://doi.org/10.1021/acsomega.4c03063
ACS Omega 2024, 9, 27578−27591

%, and a reaction time of 5.7 h. In order to confirm the predictions of the model, a real experiment was conducted. The results showed that the actual purity of methyl ester was 96.69 wt %, which was very close to the predicted purity. The transesterification process yielded a 77.6 wt % yield, and the overall biodiesel product was 76.2 wt %. However, this optimal condition demanded excessive chemical consumption and a long reaction time, resulting in increased costs for chemicals and operations. To address this issue, a commercial biodiesel standard with a purity level of 96.50 wt % methyl ester was introduced into eq 2. Regression analysis was then used to recalculate the three factors, leading to the recommended conditions of a 9.0:1 molar ratio of methanol to oil, a 75.0 wt % catalytic filament loading, and a 4.0 h reaction time. An actual experiment was performed to confirm the recommended conditions, and it was found that the methyl ester purity was 96.58 wt %, which was very close to 96.50 wt %. The transesterification process provided a 79.7 wt % biodiesel yield, with an overall product yield of 78.3 wt %. This confirms the accuracy and consistency of model eq 2 for optimizing the biodiesel production process. Table 7 summarizes both the optimal and recommended conditions from the predictive model and actual experiment. In terms of chemical consumption and reaction time, the recommended conditions could save 16.7% of the methanol content, 11.9% of the catalytic filament loading, and 42.5% of the reaction time compared to the optimal conditions. Table 8 summarizes the composition and physical properties of the biodiesel synthesized using 15 wt % CaO catalytic filaments under the recommended conditions. Additionally, Figure 8 shows the raw materials of SPO, PSPO, and biodiesel obtained via CaO catalytic filaments. For the biodiesel composition analysis, a TLC/FID analyzer was used to determine the purities of methyl ester, TG, DG, MG, and FFA. The analysis results confirmed that the methyl ester content reached 96.58 wt %, complying with Thailand's biodiesel standard. The biodiesel had a specific gravity of 0.852 at 60 °C, a dynamic viscosity of 5.43 cSt at 40 °C, a cloud point of 12 °C, a pour point of 10 °C, and an acid value of 1.2 mg KOH/g.

Table 8. Compositions and Physical Properties of SPO, PSPO, and Biodiesel

Properties	Units	SPO[24]	PSPO[24]	Biodiesel (present work)
Compositions				
Methyl ester	wt %	0.00	89.25	96.58
Triglyceride	wt %	9.80	6.93	1.55
Diglyceride	wt %	0.80	2.57	1.13
Monoglyceride	wt %	0.24	0.30	0.38
Free fatty acid	wt %	89.16	0.94	0.37
Physical properties				
Specific gravity (at 60 °C)	–	0.856	0.850	0.852
Dynamic viscosity	cSt	3.89[a]	5.36[b]	5.43[b]
Cloud point	°C	n/a	13	12
Pour point	°C	42	11	10
Acid value	mg KOH/g	197.7	1.8	1.2

[a]Dynamic viscosity at 60 °C. [b]Dynamic viscosity at 40 °C.

3.3.4. Reusability of Catalytic Filaments for Biodiesel Production from PSPO. The number of reusability cycles for catalytic filaments containing 15% CaO for the transesterification of new PSPO were determined under the recommended conditions. To validate the catalytic activity of the reused filaments, the purity of methyl ester was measured throughout each running cycle, as shown in Figure 9. Additionally, Figure 10 shows the fresh and spent CaO catalytic filaments for biodiesel production from PSPO after each transesterification cycle. The purity of the methyl ester in the biodiesel is shown in Figure 9, with the ester purities gradually decreasing after each cycle. After the second cycle, the purity of the methyl ester produced using the reused CaO catalytic filaments dropped to 95.8 wt %. Nevertheless, the purity remained above 95.0 wt % after the third cycle, and it stabilized at a lower 95.0 wt % after the fourth cycle. To evaluate the catalyst's reusability, the weight loss of catalytic filaments over successive cycles was examined. The results found that the percentages of weight losses of catalytic filaments in biodiesel reactants were 0.84, 0.77, 0.84, and 0.93 wt % for the first, second, third, and fourth cycles, respectively. Moreover, the filtrate reaction mixture was analyzed using ICP-OES to assess the calcium leaching. The observed calcium leaching during the first through the fourth cycle was 394, 410, 340, and 493 mg/kg, respectively. These leachings could contribute to the decrease in catalytic activity over several cycles.[41] Therefore, it is necessary to extrude ABS filaments with more than 15% CaO powder by weight in order to increase the number of cycles in the transesterification process. As the catalytic activity decreases with each cycle, more cycles are required to maintain a methyl ester purity of over 96.5 wt %. Therefore, this study suggests a novel approach for extruding a catalytic filament and printing a component with a high concentration of more than 15 wt % CaO powder, which could potentially increase the number of transesterification reaction cycles in future research using a catalytic reactor.

4. CONCLUSIONS

This study successfully explored the potential of combining solid CaO catalysts with ABS to form CaO catalytic filaments for use in a 3D printer. It is recommended to blend a maximum of 15 wt % of CaO catalyst content into the ABS material. The hardness and compressive strength of the composite were improved by 8.7% and 25.4%, respectively, compared to pure ABS. However, increasing CaO concentrations of 15 wt % in the ABS also led to a reduction in the tensile strength, elongation at break, flexural strength, and flexural strain by 26.4%, 75.8%, 34.1%, and 17.3%. Because of the weak bonds between the solid catalyst and the ABS material, the CaO catalytic filament composite was brittle. Despite these mechanical characteristic problems, the thermal properties of the catalytic filaments were unaffected, enabling them to be used in 3D printers and extrusion machines without affecting material quality. In the biodiesel production process, optimization using the RSM resulted in a methyl ester purity of 96.58 wt % and a product yield of 79.7 wt % under recommended conditions. Furthermore, these CaO catalytic filaments could be used with the purity remaining above 95.0 wt % after the third cycle and stabilizing at a lower 95.0 wt % after the fourth cycle. In conclusion, the use of low-cost SPO has emerged as a promising option to biodiesel feedstock. The new catalytic filaments have the ability to convert PSPO to high-purity biodiesel. This approach provides a sustainable and effective solution to biodiesel production. In future work, these catalytic filaments will be printed into other catalytic reactors

https://doi.org/10.1021/acsomega.4c03063
ACS Omega 2024, 9, 27578−27591

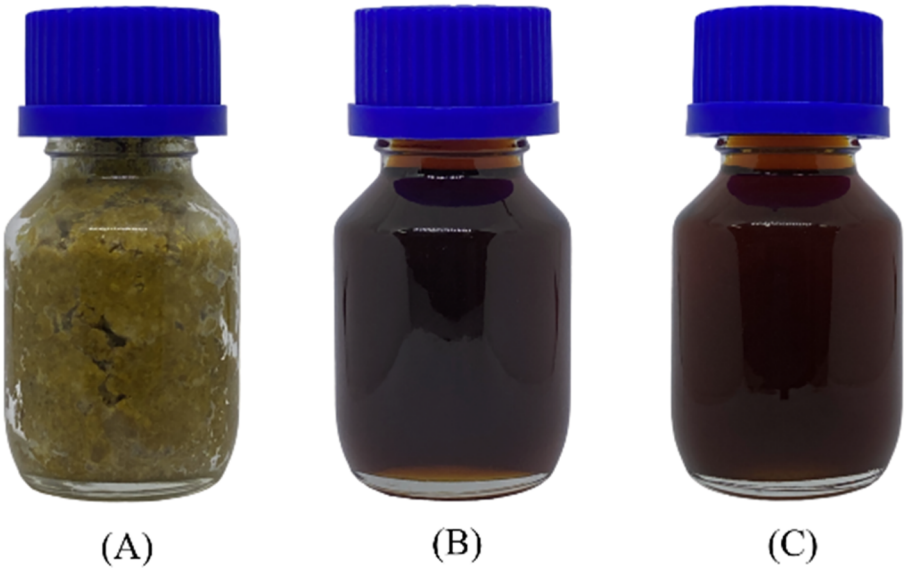

Figure 8. Raw material and product obtained via catalytic filaments: (A) raw material sludge palm oil, (B) pretreated sludge palm oil, and (C) biodiesel obtained under the recommended conditions.

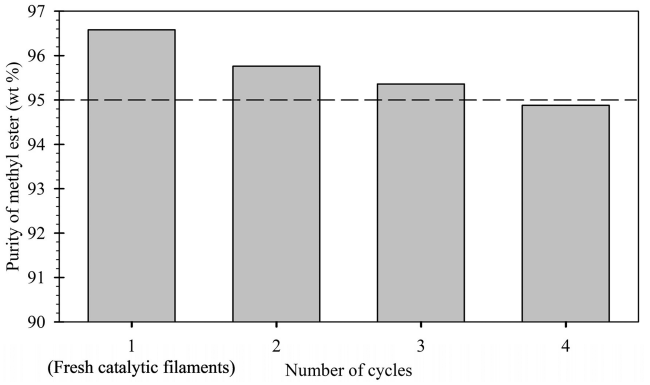

Figure 9. Purities of methyl ester from biodiesel production from PSPO using fresh CaO catalytic filaments and reused catalytic filaments after second, third, and fourth cycles.

such as static mixer reactors, microchannel reactors, and rotors in hydrodynamic cavitation reactors, to facilitate mixing and accelerate the reaction during biodiesel production. Moreover, future studies will investigate the stability of catalytic reactors over extended reaction durations, aiming to achieve more sustainable and cost-effective biodiesel production processes with less waste generation.

AUTHOR INFORMATION

Corresponding Author

Krit Somnuk − *Department of Mechanical and Mechatronics Engineering, Faculty of Engineering, Prince of Songkla University, Hat Yai, Songkhla 90110, Thailand;* orcid.org/0000-0002-1771-5120; Email: krit.s@psu.ac.th

Author

Kritsakon Pongraktham − *Department of Mechanical and Mechatronics Engineering, Faculty of Engineering, Prince of Songkla University, Hat Yai, Songkhla 90110, Thailand;* orcid.org/0000-0002-6919-0637

Complete contact information is available at: https://pubs.acs.org/10.1021/acsomega.4c03063

Notes

The authors declare no competing financial interest.

ACKNOWLEDGMENTS

This research project was supported by the National Research Council of Thailand (NRCT) (contract no. N41A650121) and the National Science, Research and Innovation Fund (NSRF) and Prince of Songkla University (ref no. ENG6701121S).

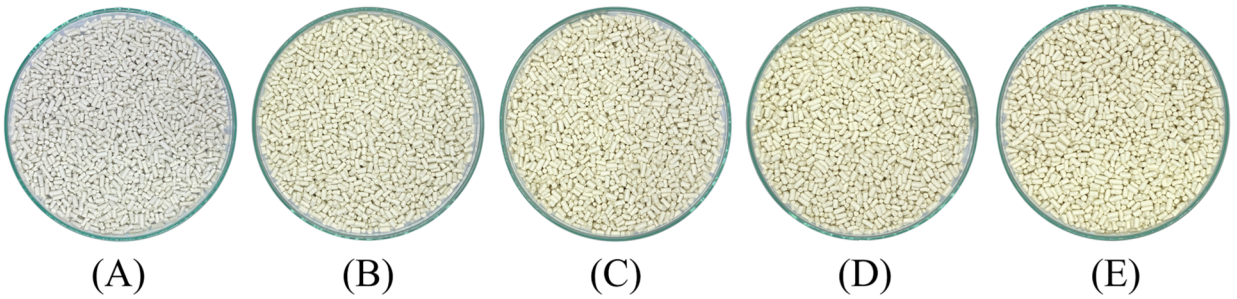

Figure 10. CaO catalytic filaments for biodiesel production from PSPO: (A) fresh catalytic filaments, and catalytic filaments after the (B) first, (C) second, (D) third, and (E) fourth cycles of the transesterification process.

https://doi.org/10.1021/acsomega.4c03063
ACS Omega 2024, 9, 27578−27591

REFERENCES

(1) Orege, J. I.; Oderinde, O.; Kifle, G. A.; Ibikunle, A. A.; Raheem, S. A.; Ejeromedoghene, O.; Okeke, E. S.; Olukowi, O. M.; Orege, O. B.; Fagbohun, E. O.; Ogundipe, T. O.; Avor, E. P.; Ajayi, O. O.; Daramola, M. O. Recent advances in heterogeneous catalysis for green biodiesel production by transesterification. *Energy Conv. Manag.* **2022**, *258*, No. 115406.

(2) Somnuk, K.; Phanyusoh, D.; Thawornprasert, J.; Oo, Y. M.; Prateepchaikul, G. Continuous ultrasound-assisted esterification and transesterification of palm fatty acid distillate for ethyl ester production. *Processes* **2021**, *9* (3), 449.

(3) Neupane, D. Biofuels from renewable sources, a potential option for biodiesel production. *Bioengineering* **2023**, *10* (1), 29.

(4) Mohiddin, M. N. B.; Tan, Y. H.; Seow, Y. X.; Kansedo, J.; Mubarak, N. M.; Abdullah, M. O.; Chan, Y. S.; Khalid, M. Evaluation on feedstock, technologies, catalyst and reactor for sustainable biodiesel production: A review. *J. Ind. Eng. Chem.* **2021**, *98*, 60−81.

(5) Abdul Hakim Shaah, M.; Hossain, M. S.; Salem Allafi, F. A.; Alsaedi, A.; Ismail, N.; Ab Kadir, M. O.; Ahmad, M. I. A review on non-edible oil as a potential feedstock for biodiesel: Physicochemical properties and production technologies. *RSC Adv.* **2021**, *11*, 25018−25037.

(6) Juera-Ong, P.; Pongraktham, K.; Oo, Y. M.; Somnuk, K. Reduction in free fatty acid concentration in sludge palm oil using heterogeneous and homogeneous catalysis: Process optimization, and reusable heterogeneous catalysts. *Catalysts* **2022**, *12* (9), 1007.

(7) Alsultan, A. G.; Asikin-Mijan, N.; Ibrahim, Z.; Yunus, R.; Razali, S. Z.; Mansir, N.; Islam, A.; Seenivasagam, S.; Taufiq-Yap, Y. H. A short review on catalyst, feedstock, modernised process, current state and challenges on biodiesel production. *Catalysts* **2021**, *11* (11), 1261.

(8) Changmai, B.; Vanlalveni, C.; Ingle, A. P.; Bhagat, R.; Rokhum, S. L. Widely used catalysts in biodiesel production: A review. *RSC Adv.* **2020**, *10*, 41625−41679.

(9) Zhang, Y.; Duan, L.; Esmaeili, H. A review on biodiesel production using various heterogeneous nanocatalysts: Operation mechanisms and performances. *Biomass Bioenerg.* **2022**, *158*, No. 106356.

(10) Nahas, L.; Dahdah, E.; Aouad, S.; El Khoury, B.; Gennequin, C.; Abi Aad, E.; Estephane, J. Highly efficient scallop seashell-derived catalyst for biodiesel production from sunflower and waste cooking oils: Reaction kinetics and effect of calcination temperature studies. *Renew. Energy* **2023**, *202*, 1086−1095.

(11) Li, H.; Wang, Y.; Ma, X.; Guo, M.; Li, Y.; Li, G.; Cui, P.; Zhou, S.; Yu, M. Synthesis of CaO/ZrO_2 based catalyst by using UiO−66(Zr) and calcium acetate for biodiesel production. *Renew. Energy* **2022**, *185*, 970−977.

(12) Navas, M. B.; Ruggera, J. F.; Lick, I. D.; Casella, M. L. A sustainable process for biodiesel production using Zn/Mg oxidic species as active, selective and reusable heterogeneous catalysts. *Bioresour. Bioprocess.* **2020**, *7*, 4.

(13) Mmusi, K. C.; Odisitse, S.; Nareetsile, F. Comparison of CaO-NPs and chicken eggshell-derived CaO in the production of biodiesel from *Schinziophyton rautanenii* (Mongongo) nut oil. *J. Chem.* **2021**, *2021*, 1−15.

(14) Di Bitonto, L.; Reynel-Ávila, H. E.; Mendoza-Castillo, D. I.; Bonilla-Petriciolet, A.; Durán-Valle, C. J.; Pastore, C. Synthesis and characterization of nanostructured calcium oxides supported onto biochar and their application as catalysts for biodiesel production. *Renew. Energy* **2020**, *160*, 52−66.

(15) Jagadeesh, P.; Puttegowda, M.; Rangappa, S. M.; Alexey, K.; Gorbatyuk, S.; Khan, A.; Doddamani, M.; Siengchin, S. A comprehensive review on 3D printing advancements in polymer composites: technologies, materials, and applications. *Int. J. Adv. Manuf. Technol.* **2022**, *121*, 127−169.

(16) Chadha, U.; Abrol, A.; Vora, N. P.; Tiwari, A.; Shanker, S. K.; Selvaraj, S. K. Performance evaluation of 3D printing technologies: A review, recent advances, current challenges, and future directions. *Prog. Addit. Manuf.* **2022**, *7*, 853−886.

(17) Kichloo, A. F.; Raina, A.; Haq, M. I. U.; Wani, M. S. Impact of carbon fiber reinforcement on mechanical and tribological behavior of 3D-printed polyethylene terephthalate glycol polymer composites—an experimental investigation. *J. Mater. Eng. Perform.* **2022**, *31*, 1021−1038.

(18) Wissamitanan, T.; Dechwayukul, C.; Kalkornsurapranee, E.; Thongruang, W. Proper blends of biodegradable polycaprolactone and natural rubber for 3D printing. *Polymers* **2020**, *12* (10), 2416.

(19) Li, B.; Zhang, S.; Zhang, L.; Gao, Y.; Xuan, F. Strain sensing behavior of FDM 3D printed carbon black filled TPU with periodic configurations and flexible substrates. *J. Manuf. Process.* **2022**, *74*, 283−295.

(20) Osman, M. A.; Atia, M. R. A. Investigation of ABS-rice straw composite feedstock filament for FDM. *Rapid Prototyping J.* **2018**, *24* (6), 1067−1075.

(21) Kottasamy, A.; Samykano, M.; Kadirgama, K.; Rahman, M.; Noor, M. M. Experimental investigation and prediction model for mechanical properties of copper-reinforced polylactic acid composites (Cu-PLA) using FDM-based 3D printing technique. *Int. J. Adv. Manuf. Technol.* **2022**, *119*, 5211−5232.

(22) Nesterenko, P. N. 3D printing in analytical chemistry: Current state and future. *Pure Appl. Chem.* **2020**, *92* (8), 1341−1355.

(23) Martin de Vidales, M. J.; Nieto-Marquez, A.; Morcuende, D.; Atanes, E.; Blaya, F.; Soriano, E.; Fernandez-Martinez, F. 3D printed floating photocatalysts for wastewater treatment. *Catal. Today* **2019**, *328*, 157−163.

(24) Pongraktham, K.; Somnuk, K. Continuous double-step acid catalyzed esterification production of sludge palm oil using 3D-printed rotational hydrodynamic cavitation reactor. *Ultrason. Sonochem.* **2023**, *95*, No. 106374.

(25) Khatibi, M.; Khorasheh, F.; Larimi, A. Biodiesel production via transesterification of canola oil in the presence of Na−K doped CaO derived from calcined eggshell. *Renew. Energy* **2021**, *163*, 1626−1636.

(26) Das, S.; Anal, J. M. H.; Kalita, P.; Saikia, L.; Rokhum, S. L. Process optimization of biodiesel production using waste snail shell as a highly active nanocatalyst. *Int. J. Energy Res.* **2023**, *2023*, 1−26.

(27) Aitlaalim, A.; Ouanji, F.; Benzaouak, A.; El Mahi, M.; Lotfi, E. M.; Kacimi, M.; Liotta, L. F. Utilization of waste grooved razor shell (GRS) as a catalyst in biodiesel production from refined and waste cooking oils. *Catalysts* **2020**, *10* (6), 703.

(28) Foroutan, R.; Mohammadi, R.; Esmaeili, H.; Mirzaee Bektashi, F.; Tamjidi, S. Transesterification of waste edible oils to biodiesel using calcium oxide@magnesium oxide nanocatalyst. *Waste Manage.* **2020**, *105*, 373−383.

(29) Oo, Y. M.; Prateepchaikul, G.; Somnuk, K. Continuous acid-catalyzed esterification using a 3D printed rotor−stator hydrodynamic cavitation reactor reduces free fatty acid content in mixed crude palm oil. *Ultrason. Sonochem.* **2021**, *72*, No. 105419.

(30) Curbell Plastics, Chemical Resistance. https://www.curbellplastics.com/wp-content/uploads/2023/03/Chemical_Resistance-Chart_curb.pdf (accessed 2024-04-24).

(31) ASTM Standard D638−14. *Standard test method for tensile properties of plastics*; ASTM International, West Conshohocken, PA, 2015.

(32) ASTM Standard D695−15. *Standard test method for compressive properties of rigid plastics*; ASTM International, West Conshohocken, PA, 2015.

(33) Adeniran, O.; Cong, W.; Bediako, E.; Aladesanmi, V. Additive manufacturing of carbon fiber reinforced plastic composites: the effect of fiber content on compressive properties. *J. Compos. Sci.* **2021**, *5* (12), 325.

(34) ASTM Standard D790−17. *Standard test methods for flexural properties of unreinforced and reinforced plastics and electrical insulating materials*; ASTM International, West Conshohocken, PA, 2017.

(35) Panneerselvam, T.; Raghuraman, S.; Vamsi Krishnan, N. Investigating mechanical properties of 3D-printed polyethylene terephthalate glycol material under fused deposition modeling. *J. Inst. Eng. India Ser. C* **2021**, *102*, 375−387.

https://doi.org/10.1021/acsomega.4c03063
ACS Omega 2024, 9, 27578−27591

(36) ASTM Standard D2240−15. *Standard test method for rubber property—durometer hardness*; ASTM International, West Conshohocken, PA, 2016.
(37) Yeh, C. H.; Chou, C. M.; Lin, C. P. Design of experiment for optimization of 3D printing parameters of base plate structures in colostomy bag for newborns. *J. Ind. Prod. Eng.* **2021**, *38* (7), 523−535.
(38) Narlıoğlu, N.; Salan, T.; Alma, M. H. Properties of 3D-printed wood sawdust-reinforced PLA composites. *BioResources* **2021**, *16* (3), 5467−5480.
(39) Hart, K. R.; Dunn, R. M.; Sietins, J. M.; Hofmeister Mock, C. M.; Mackay, M. E.; Wetzel, E. D. Increased fracture toughness of additively manufactured amorphous thermoplastics via thermal annealing. *Polymer* **2018**, *144*, 192−204.
(40) Gaide, I.; Makareviciene, V.; Sendzikiene, E. Effectiveness of eggshells as natural heterogeneous catalysts for transesterification of rapeseed oil with methanol. *Catalysts* **2022**, *12* (3), 246.
(41) Lani, N. S.; Ngadi, N.; Inuwa, I. M. New route for the synthesis of silica-supported calcium oxide catalyst in biodiesel production. *Renew. Energy* **2020**, *156*, 1266−1277.
(42) Mahmood, N. Q.; Marossy, K.; Baumli, P. Effects of nanocrystalline calcium oxide particles on mechanical, thermal, and electrical properties of EPDM rubber. *Colloid Polym. Sci.* **2021**, *299*, 1669−1682.
(43) Revert, A.; Reig, M.; Seguí, V. J.; Boronat, T.; Fombuena, V.; Balart, R. Upgrading brewer's spent grain as functional filler in polypropylene matrix. *Polym. Compos.* **2017**, *38*, 40−47.
(44) Pavon, C.; Aldas, M.; Samper, M. D.; Motoc, D. L.; Ferrandiz, S.; López-Martínez, J. Mechanical, dynamic-mechanical, thermal and decomposition behavior of 3D-printed PLA reinforced with $CaCO_3$ fillers from natural resources. *Polymers* **2022**, *14* (13), 2646.
(45) Fouly, A.; Alnaser, I. A.; Assaifan, A. K.; Abdo, H. S. Evaluating the performance of 3D-printed PLA reinforced with date pit particles for its suitability as an acetabular liner in artificial hip joints. *Polymers* **2022**, *14* (16), 3321.
(46) Kasar, A. K.; Watson, K. P.; D'Souza, B.; Menezes, P. L. Role of B_2O_3 and CaO in Al_2O_3 matrix composite: In-situ phases, density, hardness and wear resistance. *Tribol. Int.* **2022**, *172*, No. 107588.
(47) Kirubakaran, M.; Arul Mozhi Selvan, V. Experimental investigation on the effects of micro eggshell and nano-eggshell catalysts on biodiesel optimization from waste chicken fat. *Bioresource Technology Reports* **2021**, *14*, No. 100658.
(48) Chueluecha, N.; Kaewchada, A.; Jaree, A. Biodiesel synthesis using heterogeneous catalyst in a packed-microchannel. *Energy Conv. Manag.* **2017**, *141*, 145−154.
(49) Kumar, S.; Ramesh, M. R.; Doddamani, M. S.; Rangappa, M.; Siengchin, S. Mechanical characterization of 3D printed MWCNTs/HDPE nanocomposites. *Polym. Test* **2022**, *114*, No. 107703.
(50) Cao, X.; Yang, Y.; Luo, H.; Cai, X. High efficiency intumescent flame retardancy between Hexakis (4-nitrophenoxy) cyclotriphosphazene and ammonium polyphosphate on ABS. *Polym. Degrad. Stab.* **2017**, *143*, 259−265.
(51) Gomez-Caturla, J.; Montanes, N.; Quiles-Carrillo, L.; Balart, R.; Garcia-Garcia, D.; Dominici, F.; Puglia, D.; Torre, L. Development of biodegradable PLA composites and tangerine peel flour with improve toughness containing a natural-based terpenoid. *Express Polym. Lett.* **2023**, *17*, 789−805.
(52) Çantı, E.; Aydin, M. Effects of micro particle reinforcement on mechanical properties of 3D printed parts. *Rapid Prototyping J.* **2018**, *24* (1), 171−176.
(53) Borah, M. J.; Das, A.; Das, V.; Bhuyan, N.; Deka, D. Transesterification of waste cooking oil for biodiesel production catalyzed by Zn substituted waste egg shell derived CaO nanocatalyst. *Fuel* **2019**, *242*, 345−354.
(54) Krishnamurthy, K.N.; Sridhara, S.N.; Ananda Kumar, C.S. Optimization and kinetic study of biodiesel production from *Hydnocarpus wightiana* oil and dairy waste scum using snail shell CaO nano catalyst. *Renew. Energy* **2020**, *146*, 280−296.
(55) Aisien, F. A.; Aisien, E. T. Modeling and optimization of transesterification of rubber seed oil using sulfonated CaO derived from giant African land snail (*Achatina fulica*) catalyst by response surface methodology. *Renew. Energy* **2023**, *207*, 137−146.

https://doi.org/10.1021/acsomega.4c03063
ACS Omega 2024, 9, 27578−27591